

Responsivity–Resistance Relationship in MIIM Diodes

S. Brad Herner, *Member, IEEE*, Amina Belkadi, *Student Member, IEEE*, Ayendra Weerakkody, Bradley Pelz, and Garret Model, *Member, IEEE*

Abstract—The metal–insulator–insulator–metal (MIIM) systems of $\text{Co}/\text{Co}_3\text{O}_4/\text{TiO}_2/\text{Ti}$ and $\text{Ni}/\text{NiO}/\text{TiO}_2/\text{Cr}$ exhibit among the best reported combinations of the desirable quantities of high responsivity and low resistance. The relationship between responsivity and resistance in MIIM diodes is developed by fabricating and measuring hundreds of diodes of these compositions. For both diodes, higher responsivities are associated with higher resistances, which confirms a theoretical prediction for MIIM diode characteristics. Simulation of diode behavior using a transfer-matrix method diode simulator confirms the results and is consistent with nonresonant tunneling behavior.

Index Terms—Energy harvesting, metal–insulator–insulator–metal (MIIM) diode, rectennas, responsivity.

I. INTRODUCTION

WE REPORT on the relationship between responsivity and resistance in metal–insulator–insulator–metal (MIIM) diodes. These diodes are suitable for ultra-high frequency operation in optical rectennas to convert infrared radiation into electrical power [1]. Optical rectennas combine sub-micron antennas with ultra-high speed diodes to rectify incident radiation. The optical frequency signal from the antenna is rectified by the diode and flows through a low bandpass dc voltage filter to the load. This circuit acts as a diode clamp, which raises the output dc voltage to as high as the peak input ac voltage. Both metal/insulator/metal (MIM) and MIIM diodes have been investigated for this application. It is desirable to have low resistance (R) and capacitance (C) in these diodes to minimize the RC time constant of the device and to match the diode impedance to that of the antenna for efficient power transfer [2]. It is also desirable to have a large responsivity [(dc) out per unit ac power in].

However, a tradeoff between low resistance and high responsivity has been shown in MIM diodes, as large barrier heights result in high responsivity but at the expense of high resistance

Manuscript received October 13, 2017; revised November 19, 2017; accepted December 30, 2017. This work was supported by RedWave Energy. (Corresponding author: S. Brad Herner.)

S. B. Herner is with RedWave Energy, Boulder, CO 80309 USA (e-mail: brad.herner@gmail.com).

A. Belkadi, A. Weerakkody, B. Pelz, and G. Model are with the Department of Electrical, Computer, and Energy Engineering, University of Colorado, Boulder, CO 80309 USA (e-mail: amina.belkadi@colorado.edu; Don.Weerakkody@colorado.edu; brad.pelz@colorado.edu; model@colorado.edu).

Color versions of one or more of the figures in this paper are available online at <http://ieeexplore.ieee.org>.

Digital Object Identifier 10.1109/JPHOTOV.2018.2791421

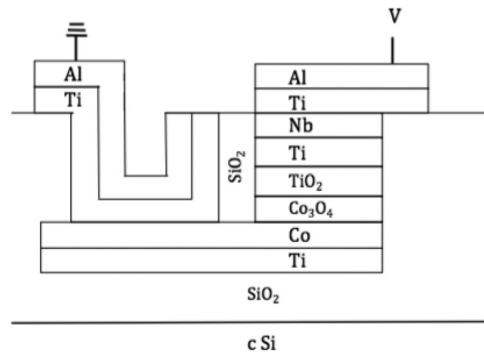


Fig. 1. Cross sectional schematic of the $\text{Co}/\text{Co}_3\text{O}_4/\text{TiO}_2/\text{Ti}$ diode.

[3], [4]. There has been a theoretical prediction that MIIM diodes could provide higher responsivities with lower resistances but it has not been verified experimentally in a systematic way [5]. We systematically fabricated and tested $\text{Co}/\text{Co}_3\text{O}_4/\text{TiO}_2/\text{Ti}$ and $\text{Ni}/\text{NiO}/\text{TiO}_2/\text{Cr}$ diodes, as these material combinations have the potential to give the low resistance required to match the antenna while providing good responsivities. In order to measure hundreds of these devices, we compare their characteristics, show the effects of annealing, establish a relationship between responsivity and resistance of MIIM diodes formed from these two materials systems, and use simulations to infer the transport mechanism.

II. FABRICATION AND CHARACTERIZATION

A. Fabrication

Diodes formed from $\text{Co}/\text{Co}_3\text{O}_4/\text{TiO}_2/\text{Ti}$ show particularly promising current–voltage characteristics. We have previously described the fabrication and initial properties of these diodes, [6] and briefly summarize the fabrication sequence here. A schematic of the device is shown in Fig. 1. Devices were fabricated on 100-mm-diameter silicon wafers coated with a SiO_2 film. Evaporated cobalt films were patterned by a lift-off process to form the lower electrode. Cobalt oxide films were grown by plasma oxidation of the metal at a power of 30 W in an O_2 environment at a pressure of 50 mtorr. The Co_3O_4 thickness was measured by variable angle spectroscopic ellipsometry and the phase was previously confirmed by X-ray photoelectron spectroscopy [6]. The TiO_2 films were deposited on the Co_3O_4 films by reactive sputtering at a pressure of 3 mtorr in an environment of 60% O_2 and 40% Ar, and a power of 60 W, for various

times. The TiO_2 film thickness was estimated by depositing a much thicker film, measuring the thickness, and extracting the deposition rate. A 5-nm-thick titanium film was evaporated onto the TiO_2 , which was followed by a 200-nm-thick sputtered niobium film. The $\text{Co}_3\text{O}_4/\text{TiO}_2/\text{Ti}/\text{Nb}$ stack was then patterned and etched into a circular pillar on top of the Co electrode.

A passivating layer of SiO_2 was deposited by plasma-enhanced chemical vapor deposition at 190°C and then partially removed by chemo-mechanical polishing, which exposes the top of the Nb pillar. Contacts to the bottom Co and upper Nb were made with Ti/Al. The resulting diode area was $0.071\ \mu\text{m}^2$ for the $\text{Co}/\text{Co}_3\text{O}_4/\text{TiO}_2/\text{Ti}$ diodes. For the $\text{Ni}/\text{NiO}/\text{TiO}_2/\text{Cr}$ diodes, the fabrication was the same with the following exceptions: A nickel film replaced the cobalt film for the lower electrode, a NiO film was also grown in an O_2 ambient, evaporated chromium was the contact to the TiO_2 film, and the passivating SiO_2 was deposited by sputtering at room temperature. Due to the use of sputtered SiO_2 for passivation, the Ni-based diodes had a lower thermal exposure *as-fabricated* compared with the Co-based diodes. The maximum temperature during Ni diode fabrication was 135°C . However, the as-fabricated $\text{Ni}/\text{NiO}/\text{TiO}_2/\text{Cr}$ diodes only became functional after they were annealed to temperatures of 200°C or greater. All other films and fabrications were the same. Due to difficulties in etch, only the larger $1\ \mu\text{m}^2$ $\text{Ni}/\text{NiO}/\text{TiO}_2/\text{Cr}$ diodes yielded working devices.

B. Characterization

Current–voltage measurement sweeps were done from -0.3 to $+0.3$ V, as the devices operate near zero bias in energy-harvesting applications. The data were fitted by a seventh-order polynomial to reduce the effects of measurement noise, which would distort the second derivative of the curve. Figures of merit for these diodes are zero-bias responsivity (ZBR), which is defined as

$$\beta_0 = \left[\frac{d^2 I}{2d^2 V} \right]_{V=0}$$

and zero bias resistance, which is defined as

$$R_D = \left[\frac{dV}{dI} \right]_{V=0}.$$

C. Results

Six wafers with different $\text{Co}_3\text{O}_4/\text{TiO}_2$ thicknesses were fabricated and measured. Fifteen to twenty-two devices were measured on each wafer with resultant median and 1 sigma distributions of responsivity and resistance calculated. Table I summarizes the values of responsivity and resistance for each wafer immediately after fabrication:

There was variation among the diodes measured, as shown in Fig. 2 by the distributions for wafer 3. These variations can arise from a variation in the diode oxide thickness.

It has been shown previously that annealing these diodes can dramatically reduce resistance along with a much smaller change in the responsivity [6]. The comparison of the as-fabricated diodes that saw a maximum temperature of 190°C with those annealed at a temperature of 255°C reveals that the

TABLE I
COMPARISON OF $\text{Co}/\text{Co}_3\text{O}_4/\text{TiO}_2/\text{Ti}$ DIODE CHARACTERISTICS
WITH VARIOUS OXIDE THICKNESS

#	Co_3O_4 (nm)	TiO_2 (nm)	Median $R_D \pm 1$ sigma @ 0 V (Ω)	Median $\beta_0 \pm 1$ sigma @ 0 V (A/W)
1	1.2	2.0	1600 ± 400	0.1 ± 0.16
2	1.4	1.6	300 ± 80	0.8 ± 0.09
3	1.4	2.0	2400 ± 1650	1.2 ± 0.18
4	1.4	2.4	$15\,000 \pm 13\,400$	0.8 ± 0.49
5	1.5	1.2	200 ± 80	0.5 ± 0.09
6	1.5	1.6	1700 ± 400	1.0 ± 0.16

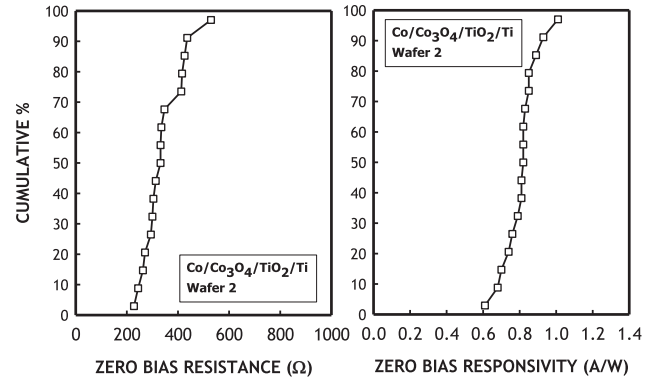


Fig. 2. Distributions of resistance (left) and responsivity (right) in actual $\text{Co}/\text{Co}_3\text{O}_4/\text{TiO}_2/\text{Ti}$ diodes from wafer 2.

responsivity decreases ~ 0.5 times, whereas the resistance decreases ~ 0.1 times, as shown in the example in Fig. 3. The origin of the resistance that decreases with annealing is unknown. Both Co_3O_4 and TiO_2 films have increased crystallinity and grain size when annealed between 175 and 300°C [7]–[10]. Both films are wide bandgap semiconductors [11], [12]. Increased grain size in polycrystalline semiconductors has been associated with decreased trap density and higher conductivity [13]. It is possible that annealing these devices has had the same effect in these films.

A scatterplot of the resistance and responsivity for all the Co-based devices measured is shown in Fig. 4. Diodes from wafers 2, 4, 5, and 6 were annealed for 10 min at 222°C in air to decrease resistance. From the scatterplot, it is apparent that the higher responsivity diodes have higher resistances. Diodes with zero bias responsivities (ZBR) greater than 1.5 A/W all had resistances greater than $1000\ \Omega$.

Even with the variation among the devices, the dotted line shows that diodes with highest responsivity necessarily come with high resistance. As compared with the results by Bean *et al.* [4] of a resistance–responsivity relationship for MIM diodes, the MIIM diode achieves higher responsivity with either a similar or lower resistance, as shown here. With resonant tunneling MIIM diodes, the responsivity increases and the resistance decreases in the low resistance range of interest, a trend that cannot be achieved with MIM diodes [5].

A second type of diode, $\text{Ni}/\text{NiO}/\text{TiO}_2/\text{Cr}$, was also studied. Single insulator diodes that are formed with Ni/NiO are desirable because the low Ni/NiO barrier results in low resistance,

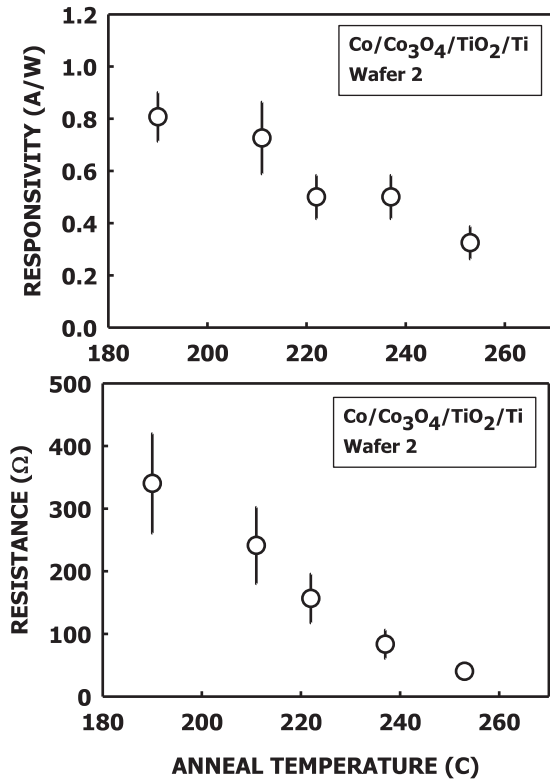


Fig. 3. Median responsivities (upper) and resistances (lower) at 0 V, with 1 sigma error bars, of actual Co/Co₃O₄/TiO₂/Ti diodes from wafer 2 after 10 min anneal in air at the temperature indicated.

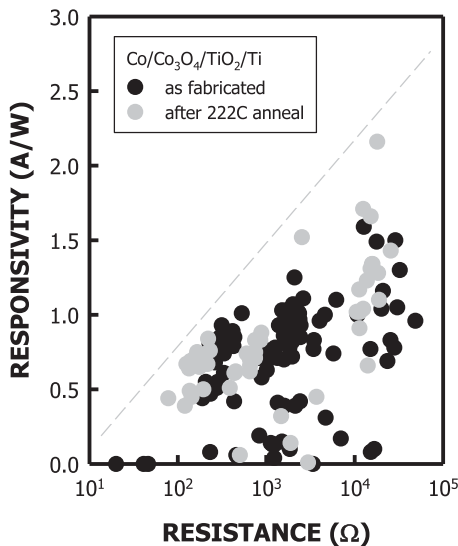


Fig. 4. Plot of resistance and responsivity at 0 V of actual 0.071 μm² Co/Co₃O₄/TiO₂/Ti diodes.

which provides a good impedance match with the antenna and a tolerable RC time constant [14]. The addition of the second insulator increases the diode responsivity.

The Ni-based diodes showed different behavior after annealing, with responsivity peaking after a 243 °C anneal, and then declining, and the resistance initially increasing up to 234 °C

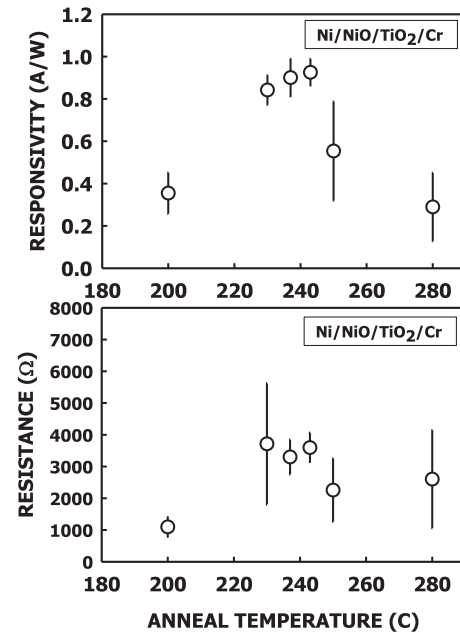


Fig. 5. Median responsivities (upper) and resistances (lower) at 0 V, with 1 sigma error bars, of actual Ni/NiO/TiO₂/Cr diodes after 10 min anneals in air at the temperature indicated.

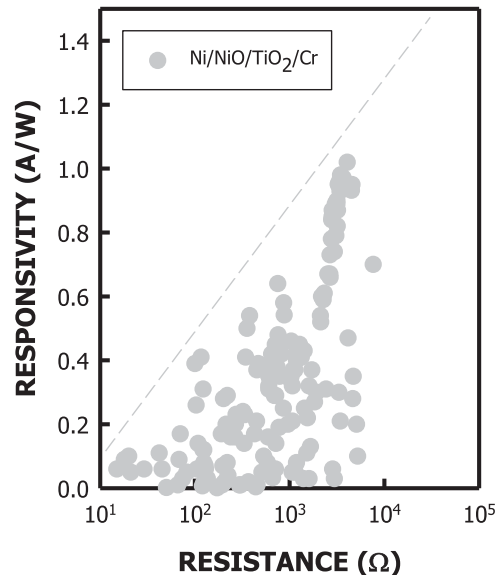


Fig. 6. Plot of resistance and responsivity at 0 V of actual 1 μm² Ni/NiO/TiO₂/Cr diodes.

and then leveling off with the increase of the anneal temperature, as shown in Fig. 5. The behavior with annealing is different than for the Co/Co₃O₄/TiO₂/Ti diodes. A scatterplot of the resistance and responsivity for the Ni/NiO/TiO₂/Cr devices is shown in Fig. 6, with all the diodes in the plot having been annealed. The Ni diodes have a similar relationship between responsivity and resistance as the Co diodes. The relationship of higher responsivity coincident with higher resistance is not unique to either diode.

TABLE II
MATERIAL PARAMETERS USED IN SIMULATION

Metal	Φ - fitted (eV)	Φ - [16] (eV)	Insulator	χ - fitted (eV)	χ (eV)
Co	4.8	5.0	Co ₃ O ₄	4.6	N/A
Ti	4.5	4.33	TiO ₂	4.2	4.1 [17]
Ni	5.0	5.04–5.35	NiO	4.9	4.9 [18]
Cr	4.4	4.5			

As the Ni-based diodes have 14 times larger cross section than that of the Co-based diodes, a fair comparison would be to normalize the resistance by increasing the Ni-based diodes' resistance by a similar amount. With normalized resistance to a cross section of $0.071 \mu\text{m}^2$, the highest responsivity Ni-based diode has a responsivity of ~ 1 A/W and a resistance of 56 k Ω , whereas the highest responsivity Co-based diode has a responsivity of 2.2 A/W and a resistance of 18 k Ω . When adjusted for area, the Co-based diodes have a higher responsivity for a given resistance compared with the Ni-based diodes.

The results from both the Co- and Ni-based diodes confirm the earlier theoretical prediction that MIIM diodes can achieve higher responsivities than MIM diodes [5]. A previous publication has compared responsivities and resistances of various MIM and MIIM diodes, normalized to the cross sectional area of the diodes [6].

D. Simulation

Using a quantum mechanical MIM diode simulator [15], the thickness of each oxide was varied to observe the responsivity–resistance relationship for both Co/Co₃O₄/TiO₂/Ti and Ni/NiO/TiO₂/Cr MIIM diodes. The parameters for the materials used in the simulation and reported literature values of same are shown in Table II. The fitted parameters are extracted from the best fit to the fabricated diodes. As the work function is a property of the surface of the metal, it is expected to vary based on crystalline face or faces as well as contamination of the surface. Differences between the fitted work functions and literature values are, therefore, expected and are within normal variation.

For the Co/Co₃O₄/TiO₂/Ti diode, the thicknesses of Co₃O₄ and TiO₂ were varied from 0.7 to 1.2 nm and 0.4 to 1.1 nm, respectively. As can be seen in Fig. 7, the simulated responsivity–resistance relationship matches the observed trend from fabricated diodes shown in Fig. 4. The dashed line is in the same location in both Figs. 4 and 7. For these Co-based MIIM diodes, step tunneling, as opposed to resonant tunneling [15], is dominant, as concluded from the simulation polarity and the responsivity–resistance trend. To achieve a reduction in resistance, the diode must switch to resonant tunneling behavior. Resonant tunneling can be attained by increasing the thickness of Co₃O₄, but due to the high barriers (0.25 eV on Co₂O₃ side and 0.33 eV on TiO₂), this requires a much thicker Co₃O₄ and high bias voltages. A similar analysis follows for the Ni-based diode. For the NiO/TiO₂ diode, the NiO and TiO₂ thicknesses were varied from 0.6 to 1.2 nm and from 1.3 to

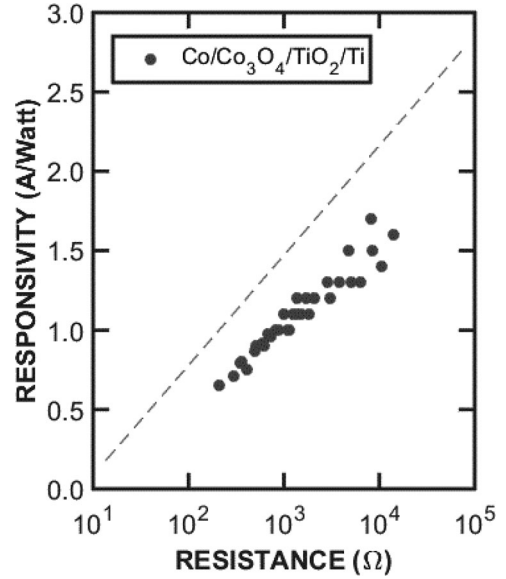


Fig. 7. Plot of resistance and responsivity at 0 V of simulated $0.071 \mu\text{m}^2$ Co/Co₃O₄/TiO₂/Ti diodes.

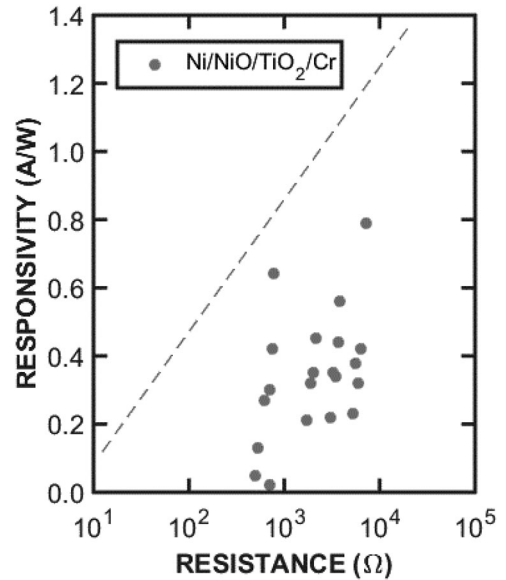


Fig. 8. Plot of resistance and responsivity at 0 V of simulated $1 \mu\text{m}^2$ Ni/NiO/TiO₂/Cr diodes.

1.7 nm, respectively. Even though the Ni/NiO barrier is lower than the Co/Co₃O₄ barrier, the thickness ratio of NiO to TiO₂ renders this as a step tunneling diode that follows a similar responsivity–resistance relationship, as shown in Fig. 8. The measured results indicate a wider variation in thickness across the wafer, which pushes the responsivity and resistance values to higher than the simulated maximum of 0.8 A/W and 7.5 k Ω and lower than the simulated minimum of 0.2 A/W and 1.7 k Ω .

There remains a desire to achieve higher responsivities with lower resistances for diodes used to rectify THz radiation. The fabrication methods and simulations of the diodes in this study

show a fundamental difficulty to achieve higher responsivity without a higher resistance. Different MIIM diode materials are necessary to achieve a higher responsivity with either similar or lower resistance.

III. CONCLUSION

We have determined in two different MIIM diodes that higher ZBR are coincident with higher resistances, which confirms earlier theoretical predictions.

Diodes made from Co/Co₃O₄/TiO₂/Ti provide higher responsivities than diodes made from Ni/NiO/TiO₂/Cr for a given resistance. Simulation of diode behavior using a transfer-matrix method diode simulator confirms the results, and is consistent with nonresonant step tunneling behavior. The substantially improved characteristics in this report compared with Bean *et al.*'s report [4] are consistent with the improvements that were simulated for double versus single insulator devices [5]. The results and simulations indicate that the MIIM diodes reported here are unlikely to produce significantly higher responsivity while maintaining a low resistance.

Another type of rectifying element, the geometric diode, may be needed to achieve higher responsivity with low resistance [19]. A geometric diode achieves IV asymmetry from the asymmetry of the physical shape of the device. The RC time constant can be significantly lower than that of either MIM or MIIM diodes. However, to achieve asymmetry in these diodes has been challenging.

ACKNOWLEDGMENT

The authors would like to thank the staff of the University of California at Santa Barbara Nanotech facility, where these devices were fabricated, and D. Doroski for help with fabrication.

REFERENCES

- [1] G. Moddel, "Will rectenna solar cells be practical?," in *Rectenna Solar Cells*. New York, NY, USA: Springer-Verlag, 2013, p. 11.
- [2] A. Sanchez, C. F. Davis, K. C. Liu, and A. Javan, "The MOM tunneling diode: Theoretical estimate of its performance at microwave and infrared frequencies," *J. Appl. Phys.*, vol. 49, pp. 5270–5277, 1978.
- [3] S. Grover and G. Moddel, "Applicability of metal/insulator/metal (MIM) diodes to solar rectennas," *IEEE J. Photovolt.*, vol. 1, no. 1, pp. 78–83, Jul. 2011.
- [4] J. A. Bean, A. Weeks, and G. D. Boreman, "Performance optimization of antenna-coupled Al/AiO_x/Pt tunnel diode infrared detectors," *IEEE J. Quantum Electron.*, vol. 47, no. 1, pp. 126–135, Jan. 2011.
- [5] S. Grover and G. Moddel, "Metal single-insulator and multi-insulator diodes for rectenna solar cells," in *Rectenna Solar Cells*. New York, NY, USA: Springer-Verlag, 2013, p. 107.
- [6] S. B. Herner, A. D. Weerakkody, A. Belkadi, and G. Moddel, "High performance MIIM diode based on cobalt oxide/titanium oxide," *Appl. Phys. Lett.*, vol. 110, 2017, Art. no. 223901.
- [7] H. Wang *et al.*, "In situ oxidation of carbon-encapsulated cobalt nanocapsules creates highly active cobalt oxide catalysts for hydrocarbon combustion," *Nature Commun.*, vol. 6, no. 1, 2015, Art. no. 7181.
- [8] X. Chen, J. P. Cheng, Q. L. Shou, F. Liu, and X.B. Zhang, "Effect of calcination temperature on the porous structure of cobalt oxide microflowers," *CrysEngComm*, vol. 14, pp. 1271–1276, 2012.
- [9] M. M. Hasan, A. S. M. A. Haseeb, R. Saidur, H. H. Masjuki, and M. Hamidi, "Influence of substrate and annealing temperatures on optical properties of RF-sputtered TiO₂ thin films," *Opt. Mater.*, vol. 32, pp. 690–695, 2010.
- [10] A. Buranawong, N. Witit-anun, and S. Chaiyakun, "Total pressure and annealing temperature effects on structure and photo-induce hydrophilicity of reactive DC sputtered TiO₂ thin films," *Eng. J.*, vol. 16, pp. 79–90, 2012.
- [11] J. Wöllenstein *et al.*, "Cobalt oxide based gas sensors on silicon substrate for operation at low temperatures," *Sensors Actuators B*, vol. 93, pp. 442–448, 2003.
- [12] F. L. English, "Capacitance and resistance measurements of TiO₂ rectifying barriers," *Solid-State Electron.*, vol. 11, pp. 473–479, 1968.
- [13] J. Levinson *et al.*, "Conductivity behavior in polycrystalline semiconductor thin film transistors," *J. Appl. Phys.*, vol. 53, pp. 1193–1202, 1982.
- [14] S. Grover and G. Moddel, "Engineering the current-voltage characteristics of metal-insulator-metal diodes using double insulator tunnel barriers," *Solid-State Electron.*, vol. 67, pp. 94–99, 2012.
- [15] C. Fumeaux, W. Herrmann, F. K. Kneubühl, and H. Rothuizen, "Nanometer thin-film Ni-NiO-Ni diodes for detection and mixing of 30 THz radiation," *Infrared Phys. Technol.*, vol. 39, no. 3, pp. 123–183, 1998.
- [16] D. R. Lide, Ed., *Handbook of Chemistry and Physics*. Boca Raton, FL, USA: CRC Press, 1993.
- [17] F. Aydinoglu *et al.*, "Higher performance metal-insulator-metal diodes using multiple insulator layers," *Austin J. Nanomed. Nanotechnol.*, vol. 1, 2013, Art. no. 1004.
- [18] P. C. D. Hobbs, R. B. Laibowitz, F. R. Libsch, N. C. LaBianca, and P. P. Chiniwalla, "Efficient waveguide-integrated tunnel junction detectors at 1.6 μm," *Opt. Express*, vol. 15, pp. 16376–16389, 2007.
- [19] Z. Zhu, S. Joshi, S. Grover, and G. Moddel, "Geometric diodes for optical antennas," in *Rectenna Solar Cells*. New York, NY, USA: Springer-Verlag, 2013, pp. 209–227.



S. Brad Herner (M'03) received the B.S. degree in materials science and engineering from the University of California, Berkeley, Berkeley, CA, USA, in 1989, the M.S. degree in engineering science from Pennsylvania State University, University Park, State College, PA, USA, in 1993, and the Ph.D. degree in materials science and engineering from the University of Florida, Gainesville, FL, USA, in 1996.

He has authored or coauthored more than 50 refereed publications and is inventor of more than 150 issued patents. His research interests include semiconductor memory, photovoltaic cells, LEDs, and rectenna solar cells.

Dr. Herner is a registered patent agent.



Amina Belkadi (S'11) received the B.S. degree in communication engineering from Khalifa University, Abu Dhabi, UAE, in 2014 and the M.S. degree in electrical engineering from the University of Colorado, Boulder, CO, USA, in 2017. She is currently working toward the Ph.D. degree in electrical engineering at the University of Colorado.

Her current research interests include the design and analysis of high-speed diodes for waste heat harvesting.



Ayendra Weerakkody received the B.Eng. and Ph.D. degrees from the University of Liverpool, Liverpool, U.K., in 2012 and 2016, respectively.

During the Ph.D. study, he worked on two emerging applications of high-k dielectrics: germanium-based MOSFETs and MIM diodes for high-frequency operation. He is currently working as a Postdoctoral Researcher with the Quantum Engineering Laboratory, University of Colorado, Boulder, CO, USA. His research interests include development and analysis of field-effect transistors, MIM diodes, and rectennas

for energy harvesting applications.



Bradley Pelz received the B.S degree in electrical engineering from Washington University in Saint Louis, Saint Louis, MO, USA, in 2010. He is currently working toward the Ph.D. degree in electrical engineering at the University of Colorado, Boulder, CO, USA.

His current research interests include the design, analysis, and experimental testing of high-speed diodes for detection and energy harvesting.



Garret Moddel (M'85) was born in Dublin, Ireland. He received the B.S. degree in electrical engineering from Stanford University, Stanford, CA, USA, in 1976, and the M.S. and Ph.D. degrees in applied physics from Harvard University, Cambridge, MA, USA, in 1978 and 1981, respectively.

After graduation, he became a founding employee with SERA Solar Corporation, a Silicon Valley photovoltaics start-up company. In 1985, he joined the University of Colorado (CU), Boulder, CO, USA, where he is currently a Professor in electrical, computer, and energy engineering. At the CU, he has developed new thin-film optoelectronic materials and devices. Currently, his research group works in quantum engineering of new thin-film metal devices for energy conversion and detection. He was the founding president and the CEO of Phiar Corporation, a venture-capital-backed high-tech start-up developing ultra-high-speed metal-insulator electronics.

Prof. Moddel was named the first CU Inventor of the Year in the Physical Sciences in 2002, and is a Fellow of the Optical Society of America.